STABILITY BEHAVIOR OF A SYNCHRONOUS-RELUCTANCE MACHINE SUPPLIED FROM A CURRENT SOURCE INVERTER

C.M. Ong
Purdue University
West Lafayette, IN

T.A. Lipo
General Electric Co.
Schenectady, NY

Summary

The development of an equivalent circuit model for a current source inverter/reluctance machine drive is described. The dynamic behavior of the basic drive with dc voltage or current source excitation is examined using linearized equations based on this model. Two forms of instability are identified which tend to limit high speed operation when dc voltage source excitation is employed. The results demonstrate the need for closed-loop control for practical implementation.

Introduction

In a related two-part paper, a review of the literature on the current source inverter (CSI) and its application potential in adjustable speed drives was presented [1]. These two papers set forth the steady-state behavior of a synchronous-reluctance machine operated from a CSI. In the application of ac drives, steady-state characteristics are not sufficient since the transient behavior of the drive is equally important to ensure reliable performance.

The stability behavior of reluctance machines fed from adjustable frequency voltage sources is well-known[2-4]. In general, instability of any ac machine supplied from a voltage source results either from inherent instability of the machine or from its interaction with the source for a given operating condition[2,5]. Machine parameters, source parameters, load characteristics and operating conditions all affect system stability. For a voltage source inverter reluctance machine drive, the influence of these parameters on stability has been investigated using a variety of methods. In the case of conventional voltage source inverters it has been found that source parameters have an adverse effect on system stability[5]. In particular, it has been established that the dc side filter capacitor must be carefully selected.

In this paper, the open-loop stability of a current source inverter reluctance machine drive is investigated. In particular, two types of dc source characteristics are investigated, namely a constant dc current and a constant dc voltage source. These two source characteristics correspond to idealized representations of a thyristor ac/dc bridge operating in the controlled-current mode and in the zero phase delay (full rectify) mode respectively. A simple equivalent circuit model of the rectifier, filter, CSI and reluctance machine is developed. The dynamic response of the system is investigated based on a linearized model derived from this equivalent circuit. Although idealized source characteristics is perhaps an oversimplification it is the intent of this paper to portray the open-loop behavior of the CSI-reluctance machine system in as simplified a manner as possible. A detailed closed-loop design approach which utilizes this open-loop model is the subject of a companion paper[6].

Description of the System

The basic system configuration of a controlled-current source inverter reluctance motor drive is shown in Fig. 1. The system consists of a controlled-rectifier dc source supplied from an ac voltage source, a dc link with a series choke, a three-phase current inverter (CSI) and a three-phase synchronous-reluctance machine. The basic circuit arrangement of the CSI using auto-sequential commutation described by Ward[7] is shown in Fig. 2. With a constant input current, the idealized output current waveform from the CSI is quasi-square[1].

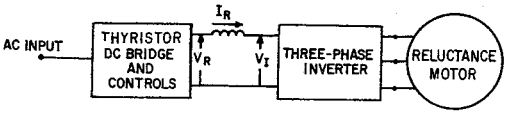

Fig. 1 Current source inverter/reluctance motor drive.

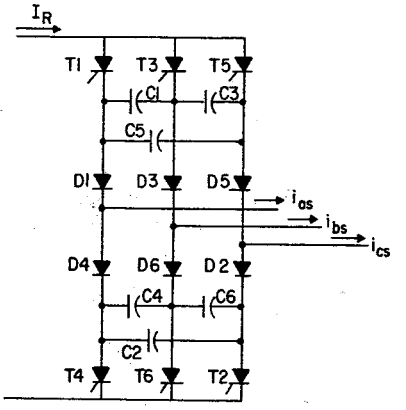

Fig. 2 Current source inverter with auto-sequential commutation.

In this paper it is assumed that:

- The CSI is a zero impedance switching device and the duration of the commutation interval can be assumed to be negligibly small.
- The reluctance machine can be represented as an idealized machine having a set of uniformly distributed stator windings. The rotor of the machine can be adequately represented by one equivalent short-circuited rotor winding in both direct and quadrature axes. The stator windings of the machine are assumed wye-connected. If necessary, delta-connected stator windings can be represented as an equivalent wye connection having identical terminal characteristics.
- The effects of saturation in the machine can be accounted for by appropriate values of saturated mutual reactance[8]. For this study, the machine parameters are assumed constant for a given operating point.
- The harmonics of the dc link current can be ignored and the resulting dc component of the dc link current has sufficiently smooth fluc-

tuations such that it can be approximated as constant throughout any inverval between two switching instants of the inverter. The validity of these simplifying approximations are clearly influenced by the inductance of the choke and the harmonics present in the dc rectifier voltage for a given operating condition.

Machine Representation

It is common in machine analysis to express the variables of an ac machine in dq0 components referred to one or more of the following reference frames,

- the stationary reference frame
- the synchronously rotating reference frame
- the reference frame fixed on the rotor.

The time reference of these reference frames is generally taken with respect to the instant the d-axis of the synchronously rotating reference frame is aligned with the axis of the phase 'a' winding of the machine. For machines with asymmetrical rotor structures, simlification is gained by referring the variables of the machine to the reference frame fixed on the rotor. Following the usual convention, the d-axis of that reference frame is aligned with the path of minimum reluctance on the rotor. However, since current rather than voltage is considered as the independent variable, it is convenient in this case to orient the d-axes of the above-mentioned reference frames with the axis of phase 'a' as shown in Fig. 3[1].

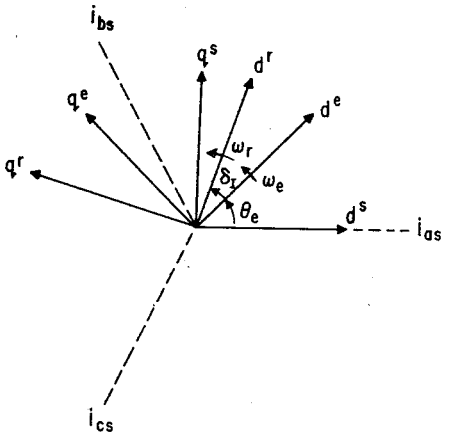

Fig 3 Axes of reference.

When a wye-connected three-phase stator winding is supplied from a balanced three-phase, three-wire ac source, the instantaneous phase voltages and currents respectively sum to zero.

$$v_{as} + v_{bs} + v_{cs} = 0 \tag{1}$$

$$i_{as} + i_{bs} + i_{cs} = 0 \tag{2}$$

As a result, the zero sequence components of these variables are not present. The transformation of the dq components of voltages and currents from the stationary reference frame to the synchronously rotating reference frame is given by the matrix $\underline{T}(\theta_e)$ where $\theta_e=\omega_e t$[1]

$$\underline{T}(\theta_e) = \begin{bmatrix} \cos\theta_e & \sin\theta_e \\ -\sin\theta_e & \cos\theta_e \end{bmatrix} \tag{3}$$

Also, from Fig. 3, the transformation of dq variables in the synchronously rotating reference frame to the reference frame fixed on the rotor $\underline{T}(\delta_I)$ is given by the same transformation matrix but with δ_I replacing θ_e in the corresponding trigonometric terms of Eq. 3. It should be noted that the angle δ_I as defined by Fig. 3, although related to torque, is different than the conventional torque angle for a voltage source. The voltage and torque expressions which describe the three-phase synchronous-reluctance machine having two mutually orthogonal rotor windings are those set forth in Refs. 1 and 2 and will not be repeated here.

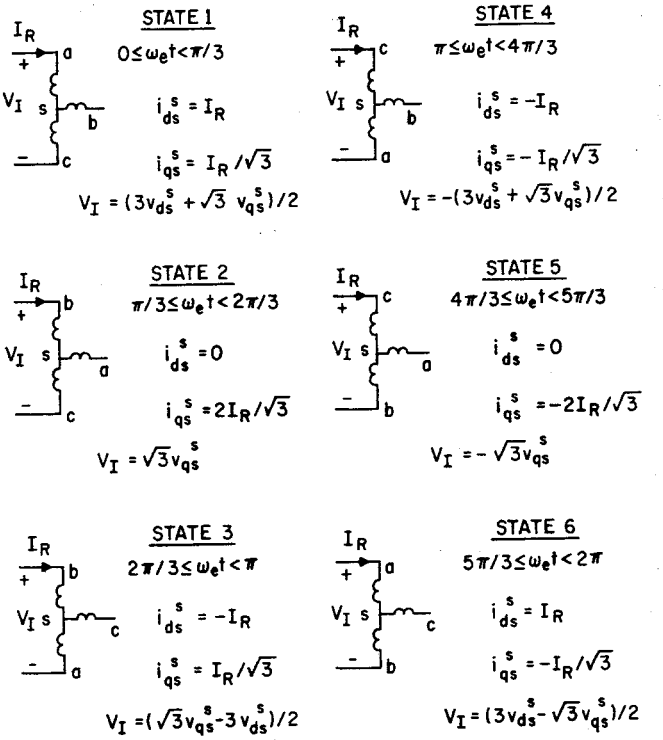

Fig. 4 The six inverter states and resulting d-q axes voltages and currents.

CSI Terminal Relations

Assuming that the CSI is an ideal lossless switching device with negligible commutation time, the sequence of current paths through the stator windings of the machine over a complete switching cycle is shown in Fig. 4. For each conduction state shown the ac phase voltages and currents can be expressed in terms of the inverter terminal voltage V_I and the rectifier current I_R. When expanded in a Fourier series these currents can be expressed

$$i_{ds}^s = \frac{2\sqrt{3}}{\pi} I_R \left[\cos\omega_e t - \frac{\cos 5\omega_e t}{5} + \frac{\cos 7\omega_e t}{7} - \frac{\cos 11\omega_e t}{11} + \cdots \right] \tag{4}$$

$$i_{qs}^s = \frac{2\sqrt{3}}{\pi} I_R \left[\sin\omega_e t + \frac{\sin 5\omega_e t}{5} + \frac{\sin 7\omega_e t}{7} + \frac{\sin 11\omega_e t}{11} + \cdots \right] \tag{5}$$

Note that Eqs. 4 and 5 are general and valid even if I_R is not a constant.

For brevity, it is convenient to define the switching functions

$$g_{ds}^{s} = \left[\cos\omega_e t - \frac{\cos 5\omega_e t}{5} + \frac{\cos 7\omega_e t}{7} - \frac{\cos 11\omega_e t}{11} + \ldots\right] \quad (6)$$

$$g_{qs}^{s} = \left[\sin\omega_e t + \frac{\sin 5\omega_e t}{5} + \frac{\sin 7\omega_e t}{7} + \frac{\sin 11\omega_e t}{11} + \ldots\right] \quad (7)$$

and also

$$I_R' = \frac{2\sqrt{3}}{\pi} I_R \quad (8)$$

The stator currents i_{ds}^{s} and i_{qs}^{s} can then be written in the form

$$i_{ds}^{s} = I_R' g_{ds}^{s} \quad (9)$$

$$i_{qs}^{s} = I_R' g_{qs}^{s} \quad (10)$$

The inverter terminal voltage can also be related to the switching functions. An inspection of the expressions for inverter terminal voltage V_I summarized in Fig. 4 will reveal that

$$V_I' = \left(v_{ds}^{s}\, g_{ds}^{s} + v_{qs}^{s}\, g_{qs}^{s}\right)$$

where

$$V_I' = \frac{\pi}{3\sqrt{3}} V_I \quad (11)$$

Since the power flow into the inverter is expressed as the product of the rectifier current and the inverter terminal voltage

$$V_I I_R = \frac{3\sqrt{3}}{\pi} I_R \left(v_{ds}^{s}\, g_{ds}^{s} + v_{qs}^{s}\, g_{qs}^{s}\right) \quad (12)$$

Substituting for $I_R g_{ds}^{s}$ and $I_R g_{qs}^{s}$ in the above expression, results in

$$V_I I_R = \frac{3}{2}\left(v_{ds}^{s}\, i_{ds}^{s} + v_{qs}^{s}\, i_{qs}^{s}\right) \quad (13)$$

Note that the left-hand side of Eq. 13 is the dc power into the CSI and the right-hand side is the power flow into the machine, thus, the result is consistent with the assumption that the CSI is a lossless switching device. Referring to Fig. 2 it can be shown that the normalized rectifier voltage V_R' may be expressed in terms of the inverter voltage V_I' and the current I_R' as

$$V_R' = V_I' + \left(R_F' + \frac{p}{\omega_b} X_F'\right) I_R' \quad (14)$$

where ω_b is the base frequency, p denotes the operator $\frac{d}{dt}$ and

$$V_R' = \frac{\pi}{3\sqrt{3}} V_R,\quad R_F' = \frac{\pi^2}{18} R_F,\quad X_F' = \frac{\pi^2}{18}\omega_b L_F .$$

An Equivalent Circuit Model

Frequently in the analysis of uniform airgap machines, i.e., induction machines, it is found convenient to refer the variables of the machine to the synchronously rotating reference frame. In general, the synchronously rotating frame is defined as that reference frame which rotates at the angular velocity of the fundamental component of the excitation vector.

Applying the transformation $\underline{T}(\theta_e)$, Eq. 3, to the stator currents i_{ds}^{s} and i_{qs}^{s} given by Eqs. 9 and 10, the corresponding dq currents in the synchronously rotating reference frame i_{ds}^{e} and i_{qs}^{e} are

$$i_{ds}^{e} = I_R' g_{ds}^{e} \quad (15)$$

$$i_{qs}^{e} = I_R' g_{qs}^{e} \quad (16)$$

where

$$\begin{bmatrix} g_{ds}^{e} \\ g_{qs}^{e} \end{bmatrix} = \underline{T}(\theta_e) \begin{bmatrix} g_{ds}^{s} \\ g_{qs}^{s} \end{bmatrix} \quad (17)$$

Similarly, it can be shown that

$$V_I' = v_{ds}^{e}\, g_{ds}^{e} + v_{qs}^{e}\, g_{qs}^{e} \quad (18)$$

When expressed explicitly as a function of time, the functions g_{ds}^{e} and g_{qs}^{e} are given by

$$g_{ds}^{e} = 1 - \frac{2}{35}\cos 6\omega_e t - \frac{2}{143}\cos 12\omega_e t - \ldots \quad (19)$$

$$g_{qs}^{e} = \frac{12}{35}\sin 6\omega_e t + \frac{24}{143}\sin 12\omega_e t + \ldots \quad (20)$$

It is clear that the constant term of g_{ds}^{e} in Eq. 19 corresponds to the fundamental component of the resultant voltage or current waveform in the stationary reference frame. The 'g' functions defined by Eqs. 6, 7, 19 and 20 are plotted in Fig. 5. When I_R is constant it is clear that these functions also effectively define the waveshape of the d-q stator currents.

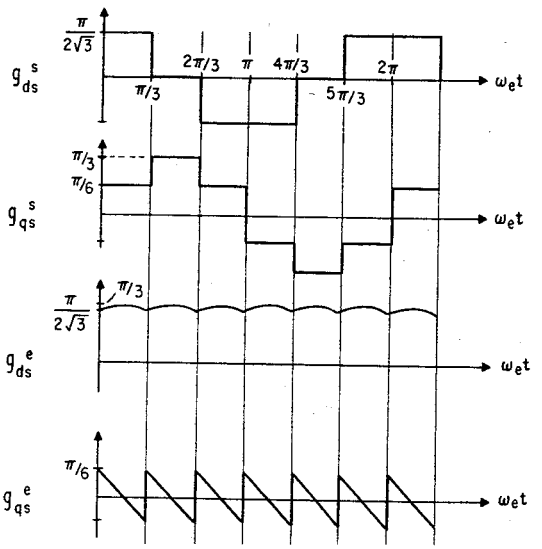

Fig. 5 The d- and q- axes switching functions.

Because the airgap of a reluctance machine is not uniform, the airgap flux density is not proportional to the MMF at every point in the gap. Hence, the self and mutual inductances of the stator windings are functions of angular position of the rotor. Voltage and current variables of the machine must be referred to a reference frame fixed on the rotor in order that the equations

relating these variables become independent of rotor position. A transformation of variables from the synchronously rotating reference frame to a reference frame fixed on the rotor can be accomplished with the aid of the transformation matrix $\underline{T}(\delta_I)$. An equivalent circuit model of both current source inverter and reluctance machine is shown in Fig. 6. Consistent with previous papers,[10] it is assumed that the time derivative operator in Fig. 6 is p/ω_b. Note that since the synchronously rotating axes have been located relative to the stator current, the torque angle δ_I is consistent with Fig. 3.

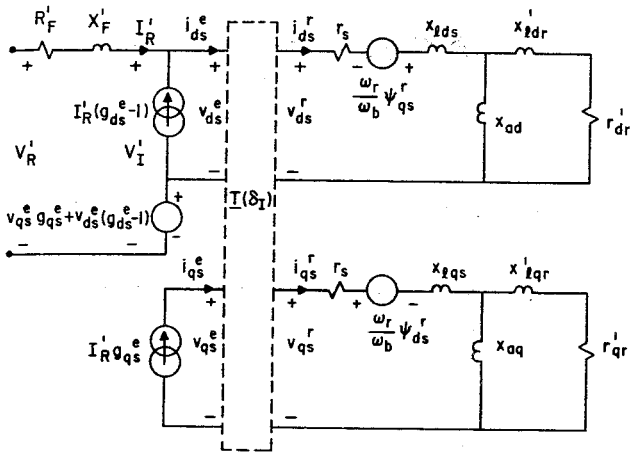

Fig. 6 A d-q axes equivalent circuit of a current source inverter/reluctance motor drive.

Small Signal Stability Behavior

The reluctance machine is, in general, described by a set of nonlinear differential equations for which no analytical solution is yet available. For the purpost of a stability investigation, a linearized system model is generally employed. Clearly, an analysis based on linearization of the set of nonlinear equations of the machine is valid only when small perturbations about an operating point is considered. In spite of this limitation, however, such linear analyses have been found to be invaluable in predicting small-disturbance transient response and in establishing guidelines for design modifications.

It was observed from the steady-state solution that harmonic components are present in the current and torque waveforms, whereas the waveforms of the phase voltages are nearly sinusoidal[1]. Reports of previous stability investigations of ac machines supplied from voltage source inverters indicate that the harmonic components do not significantly affect stability behavior[2-5]. It has been shown that the resultant contribution from the harmonics to energy conversion is small, even though the torque pulsations may be considerable. Although harmonics do contribute some additional damping, no satisfactory quantitive theory is yet available so that provision for refinement must ultimately be based on an experimental study. Hence, for simplicity the effects of harmonics will be neglected in this analysis and also in the subsequent analytical design[6].

Neglecting harmonics the 'g' functions defined by Eqs. 19 and 20 are, approximately

$$g^e_{ds} \cong 1 \tag{21}$$

$$g^e_{qs} \cong 0 \tag{22}$$

Thus, Eqs. 15 and 16 and 18 reduce to the form

$$i^e_{ds} \cong I'_R \tag{23}$$

$$i^e_{qs} \cong 0 \tag{24}$$

Replacing g^e_{ds} and g^e_{qs} in Fig. 5 by their approximate values leads to the simplified equivalent circuit shown in Fig. 7. This equivalent circuit representation clearly demonstrates the mechanism of power transfer through the dc link to the machine which, for unidirectional rectifier current, is dependent on the inverter terminal voltage, $V'_I = v^e_{ds}$, where v^e_{ds} assumes positive values for motor action and is negative for generator operation. System stability information may now be obtained by perturbing the differential equation defining Fig. 7. The inverter terminal voltage v^e_{ds} and also the currents i^r_{ds} and i^r_{qs} are dependent on the load angle δ_I. The perturbation equations, given in Appendix I, may be established from the system equations in a straightforward manner. These linear, time-invariant equations can be arranged into the state variable matrix form as given by Eq. 33. The small-signal stability behavior of the drive is investigated by evaluating the eigenvalues of this linear system of equations. To facilitate a comparison between the stability behavior exhibited by a reluctance machine supplied by a voltage inverter source and from a CSI, the machine parameters employed are similar to those used in previous studies.[1,2] These machine parameters are summarized in Appendix II.

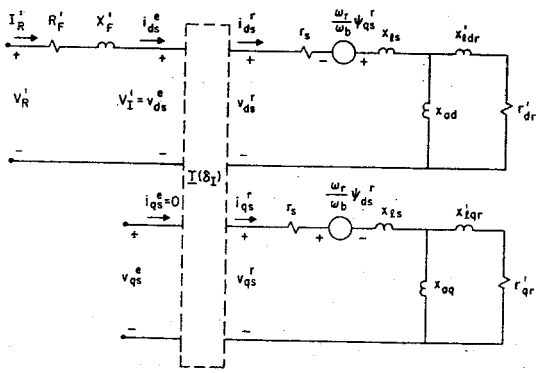

Fig. 7 Simplified d-q axes equivalent circuit.

Constant Current Source Operation

When source harmonics are neglected it can be noted from Fig. 7 that $i^e_{qs} = 0$. Hence, its perturbation Δi^e_{qs} is always zero so that the order of the system becomes one less than for an equivalent voltage source inverter. Also, for a constant current rectifier source, $\Delta I'_R = \Delta i^e_{ds} = 0$. The order of the system is therefore four when the motor is supplied from a fixed current source. System stability can be determined by calculating the system eigenvalues using Eq. 33. A typical set of system eigenvalues consists of two real and one complex pair of roots. In general, when dc link current is held constant, the machine has been found to be stable for all motoring and generating conditions which do not exceed the pull-out torque. The result agrees with previous investigators who indicated that a conventional synchronous motor is stable for fixed sinusoidal current

excitation.[9] In addition, it has been observed from the eigenvalue analysis that identical sets of eigenvalues are always obtained for equal motoring and generation torque indicating that transient response in the motoring and generating regions are identical.

Because many important motor and system parameters can often be specified by the designer, the influence of system parameters and operating conditions on stability is often an invaluable aid to design. Although space limitations prevent treating the subject exhaustimely, comparison of ovserved trends with results from a study of reluctance machines fed from voltage inverter sources are of interest.[2] The most significant parameters affecting transient behavior are:

- A reduced level of current excitation results in a higher overshoot but better damping.
- An increase in rotor inertia tends to lower the transient response frequency and, for the operating conditions investigated an improvement in the damping occurs. This result is in contrast to previous work involving voltage excitation.[3]
- Changes in the stator winding resistance and leakage reactance do not affect the transient response behavior, as can be anticipated with a constant current source excitation. Even in the case of an approximate current source, the effects due to changes in value of these stator parameters will normally be masked by the large source impedance.
- A higher resistance to leakage reactance ratio (r/x_ℓ) in the d- or q-axis rotor windings tends to improve the damping when the machine is on load. However, for no-load conditions, a higher (r/x_ℓ) ratio in the d-axis rotor winding does not affect damping. Nevertheless, a higher (r/x_ℓ) ratio in the q-axis rotor winding provides additional damping even when the machine is operating on no-load.
- A decrease in rotor saliency (x_{ad}/x_{aq}) results in a lower damped natural frequency together with improved damping.
- Finally, an increase in loading on the machine always tends to improve damping.

In order to verify these conclusions, an analog computer study was performed wherein all of the relevant system non-linearities were preserved and the CSI represented in complete detail. Computer traces of key system variables are shown in Fig. 8 for a step change in applied torque. Figures 8a and 8b indicate response for step changes in load torque from no-load to 0.2 pu motoring and 0.2 pu generating operation respectively. Note that, as predicted, the transient responses are identical except for the changes in sign. Since transient responses are identical in both regions, only the transient response in the motoring region are shown in subsequent traces.

Figure 8c illustrates the conclusion that for reduced current excitation, a higher overshoot occurs followed by a better damped response. Smaller inertia results in a higher transient response frequency and noticeable speed fluctuations as portrayed in Fig. 8d. Hence, a larger inertia enhances relative stability, although this may not be true for all operating conditions. Figure 8e shows the traces for the case of reduced rotor saliency, which has the equivalent effect of a higher load angle operation. It is observed that the response is relatively less oscillatory and because

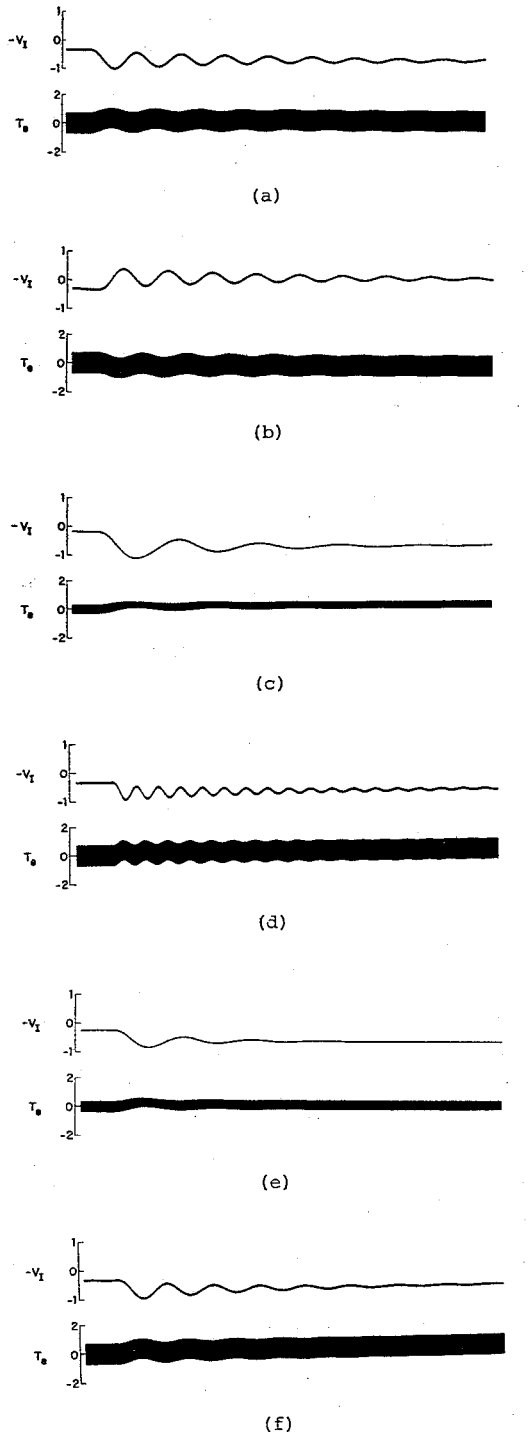

Fig. 8 Step response for constant current source excitation, I_R=0.8 (except c), f_R= 1.0, T_L=±0.2. Motor parameters are in Appendix II except as noted; (c) I_R=0.5, (d) H = 0.1 s., (e) x_{ad}=1.5, (f) r'_{qr}=0.045.

of the smaller saliency ratio, the torque pulsation is also correspondingly smaller. Figure 8f illustrates the effect of higher rotor resistances. In particular, note that a higher q-axis rotor winding resistance results in greater damping. Since these analog computer traces have been obtained with a detailed representa-

tion of the reluctance machine with non-linearities and harmonics taken into account they clearly justify the assumptions made in the small signal eigenvalue analysis.

Constant Voltage Source Operation

In many practical applications, limitations in KVA rating necessitate that the ac-dc thyristor bridge be permitted to "saturate" when motor speed exceeds a specified value of operation above a certain inverter output frequency. This mode of operation corresponds to constant horsepower operation and is analogous to the field weakening mode in conventional dc motor drives. Since operation from a voltage source is typical for many wide speed applications, it is of interest to examine the consequences of operation under such a condition. In this analysis the voltage variation of the ac supply is not considered. It will be assumed herein that for the drive under consideration, the assumption of an infinite ac busbar is justified so that $\Delta V_R = 0$. Under such conditions, the rectifier is assumed to operate without phase angle delay. If necessary, the effects of finite source impedance can be lumped with the filter choke parameters.

Stability of the CSI/reluctance motor drive operating from a voltage source is again defined by Eq. 33 where, in this case, $\Delta i_{ds}^{e} \neq 0$. In contrast to operation from a current source, the reluctance motor exhibits regions of unstable behavior when the CSI is supplied from a voltage source. Figures 9a and 9b show the boundaries between stable and unstable regions of operation as a function of the per unit frequency f_R. The operating condition assumes a fixed value of rectifier voltage which, for each frequency, provides 0.8 pu current excitation at no-load. In Fig. 9(a), an arbitrarily large value of choke inductance, 50 pu, has been selected so as to approximate the current source condition. In Fig. 9(b) a more practical value, X_F=1.2 pu has been chosen. It is interesting to note that the two widely different values of choke inductance has no discernable effect on stability behavior in the motoring region. Subsequent investigation of steady-state behavior has indicated that these boundary curves can also be predicted from considerations of steady-state power transfer (Appendix III). Hence, the result is an inherent characteristic of the system and indicates that stable operation is not possible without voltage control of the ac/dc thyristor bridge. The instability boundary in the generating region is clearly dependent on filter parameters and corresponds to a dynamic instability analogous to those which occur for conventional voltage source operation.

The forms of instability for the operating conditions labled 'b' and 'c' in Fig. 9(b) are illustrated by traces from an analog computer simulation study. Figure 10(a) shows the response following a step change of load torque from an initial (stable) operating point 'a' (T_{eo} = 0, f_R= 1.0) to an operating point labeled 'b' (T_{eo} = 0.1, f_R= 1.0). The decay of the rectifier current and torque indicates that a stable steady-state operating condition does not exist at point 'b'. Similarly, Fig. 10(b) is for a step change of load torque from operating point 'a' to a generating condition at point 'c'(T_{eo} = -0.1, f_R= 1.0). Operating point 'c' is outside the region of stable operation where net system damping becomes negative and the response diverges. Note that the speed of the machine oscillates about synchronous speed instead of the gradual decay observed for motor operation, point 'b'. The operating conditions in Fig. 9 are for fixed values of rectifier voltage corresponding to rated excitation current. In this case the rectifier output voltage and region of stability is small. Nevertheless, these results are the same regardless of the voltage level.

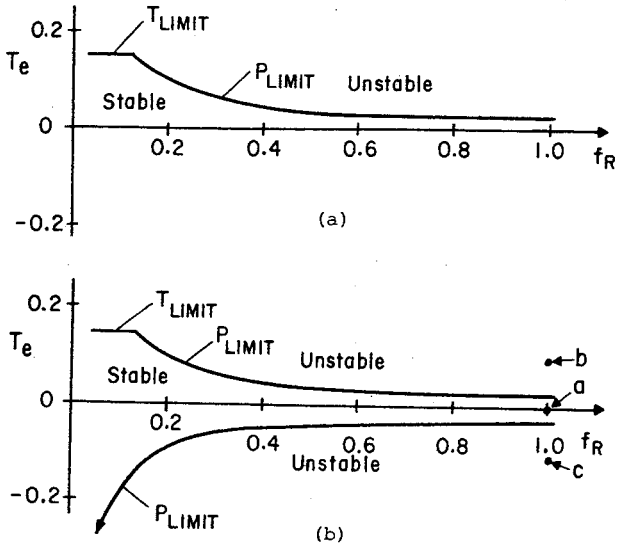

Fig. 9 Stability boundary of CSI/reluctance motor drive with constant dc rectifier voltage, (a) X_F =50, (b) X_F=1.2.

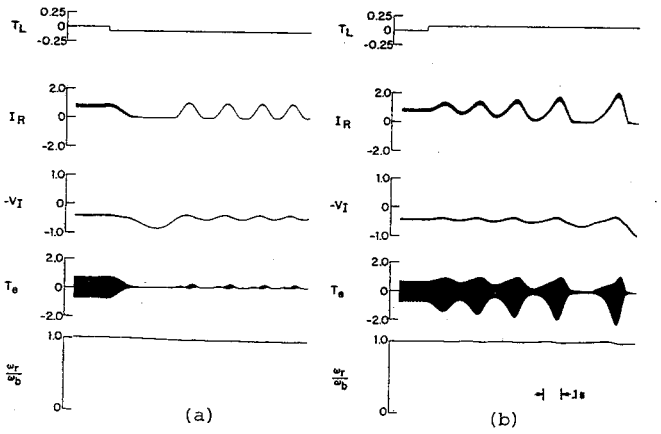

Fig. 10 Load torque switching for constant dc voltage operation, f_R = 1.0. Step change in load torque, (a) 0 to 0.1 pu, (b) 0 to -0.1 pu.

Although difficult to achieve practically, an examination of other operating conditions are also of interest. Figure 11 shows a larger region of stable operation when the rectifier voltage is adjusted so as to produce a fixed value of current excitation, I_R= 0.8 pu, independent of steady-state load and operating frequency. Hence, this mode of operation can be considered as the open loop equivalent of a voltage source adjusted to appear identical, on a steady-state basis, to a current source. It is apparent that dynamic behavior is entirely different from a conventional voltage source even though the steady-state operating point is identical. Again, a real pole moves into the right-haof plane in the motoring region. The mechanism leading to this instability is again the limitation in power transfer from rectifier to machine although this limit now occurs at somewhat higher values of torque (power). Again, a pair of complex poles moves into the right-half plane for generator operation, predicting growing oscillations. Presence of the unstable generating region is again due to insufficient damping.

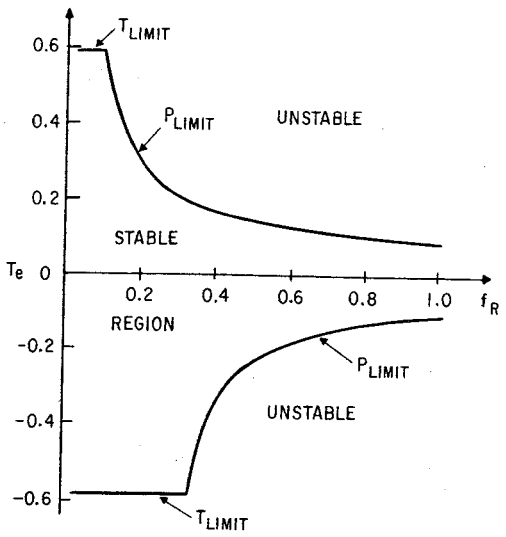

Fig. 11 Stability boundary with fixed dc rectifier voltage and steady-state current $I_R = 0.8$.

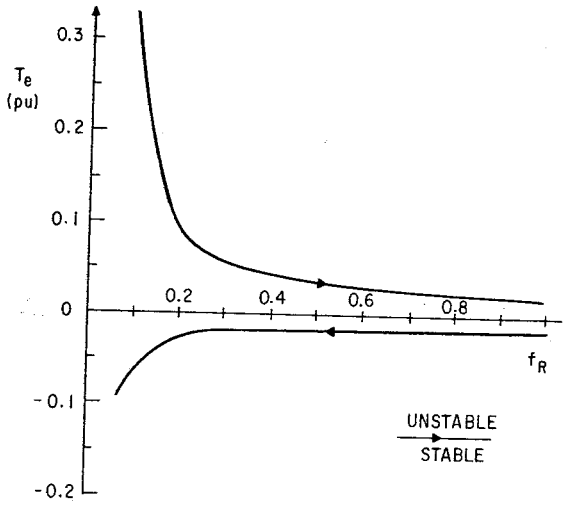

Fig. 12 Stability boundary with fixed dc rectifier voltage. Air gap flux maintained at one per unit.

Another typical operating constraint is to maintain air gap flux constant independent of load and operating frequency. Figure 12 shows the regions of stable and unstable operation when rectifier voltage is adjusted and then held constant so as to maintain rated stator flux at the specified load condition. Similar observations about the mechanisms of instability can be made.

In contrast to conventional voltage inverter operation[2] it has been established that changes in motor parameters have only relatively minor effects on the two instability modes. A study of parameter variations similar to Ref. 2 was not deemed necessary. These results point to the need for closed loop control to provide the necessary system damping. The closed loop design of such a system is the subject of a companion paper.

Conclusion

In this paper, a derivation of an equivalent circuit model of a current source inverter (CSI)/reluctance motor drive has been presented. The introduction of switching functions (g functions) have been shown to facilitate the identification of fundamental and harmonics components generated by the switching operations of the CSI, thus providing a ready means of isolating their respective contributions. When the effects of harmonic components are ignored, the equivalent circuit model leads directly to a simplified equivalent circuit model from which small displacement equations may be obtained by linearization.

Many drive system require feedback control to ensure stability. However, before design of the necessary feedback loops a stability analysis of the basic open-loop system is useful since it can often be used to establish guidelines for improving system response. Although idealized constant current and constant voltage dc source characteristics have been investigated a number of interesting results have been obtained. In particular it was found that the dc source characteristic has a dominant effect on stability and transient behavior. With a stiff current source, the CSI and reluctance machine system is unconditionally stable, whereas with a weak current source (voltage source) the same system has a much poorer stability profile.

From a stability point of view a CSI/reluctance motor drive clearly operates best when supplied from a constant current source. However, when the drive is considered as a whole, a source characteristic of this type is not necessarily desirable despite the attractiveness of an unconditionally stable system. Based on steady-state characteristics,[1] fixed dc link current operation leads to excessive voltage stresses on the inverter thyristors at light load and has the operational disadvantage of overexcitation and consequent higher torque pulsations and losses. On the other hand, open loop operation of the basic system with constant rectifier voltage has limited practical utility because of the restricted region of stable operation. It is apparent that the characteristics of a properly regulated dc current source would be a reasonable compromise. The application of the results of this paper to the closed-loop design of an adjustable speed CSI/reluctance motor drive are described in a companion paper.[6]

List of Symbols

All quantities are in per unit unless noted

Symbol	
V_R	rectifier dc terminal voltage
I_R	rectifier dc output current
V_I	inverter terminal voltage
v_{as}	phase a voltage of machine
i_{as}	phase a current of machine
v_{ds}, v_{qs}	stator voltages in d- and q-axis circuits
i_{ds}, i_{qs}	stator currents in d- and q-axis circuits
i_{dr}, i_{qr}	rotor currents in d- and q-axis circuits
ψ_{ds}, ψ_{qs}	stator flux linkages of d- and q-axis circuits
ψ_{dr}, ψ_{qr}	rotor flux linkages of d- and q-axis circuits
T_e	electromagnetic torque

T_L	load torque
ω_b	base electrical angular frequency in rad/s
ω_e	electrical angular frequency of the inverter (fundamental component) in rad/s
ω_r	rotor electrical angular frequency in rad/s
f_R	frequency ratio ω_e/ω_b
δ_I or δ	load angle for current source in rad
H	inertia constant of rotor in sec
x_{ds}, x_{qs}	synchronous reactances in the d- and q-axis circuits at base frequency
x_{ad}, x_{aq}	stator-rotor mutual reactances in the d- and q-axis at base frequency circuits
$x_{\ell s}$	stator leakage reactance at base frequency
$x_{\ell dr}$, $x_{\ell qr}$	rotor circuit leakage reactances in d- and q-axis circuits at base frequency
r_s	stator resistance
r_{dr}, r_{qr}	rotor resistances in the d- and q-axis circuits
L_F, R_F	filter inductance and resistance
p	differential operator d/dt
s	Laplace variable
t	time

Superscripts

s	to indicate a variable referred to the stationary reference frame
e	to indicate a variable referred to the synchronously rotating reference frame
r	to indicate a variable referred to the reference frame fixed to the rotor
'	to indicate a rotor parameter referred to the stator or as otherwise defined in the text

Subscript

o	to indicate the steady-state portion of the variable

Prefix

$\Delta(\ )$	to denote a small change of the variable

References

(1) Ong, C.M., Lipo, T.A., "Steady-State Analysis of a Current Source Inverter/Reluctance Motor Drive, Part I - Analysis and Part II - Experimental and Analytical Results", to be presented at the 1975 IEEE-IAS Annual Meeting, Sept. 28-Oct. 2, 1975.

(2) Lipo, T.A. and Krause, P.C., "Stability Analysis of a Reluctance Synchronous Machine", IEEE Trans. PAS, Vol. 86, 1967, pp. 825-834.

(3) Lawrenson, P.J. and Bowes, S.R., "Stability of Reluctance Machines", Proc. IEE, Vol. 117, No. 2, Feb. 1971, pp. 356-369.

(4) Cruickshank, A.J.O., Anderson, A.F., and Menzies, R.W., "Theory and Performance of Reluctance Motors with Axially Laminated Anisotropic Rotors", Proc. IEE, Vol. 118, No. 7, July 1971.

(5) Lipo, T.A. and Krause, P.C., "Stability Analysis of a Rectifier-Inverter Induction Motor Drive", IEEE Trans. on Power Apparatus and Systems, Vol. PAS-88, No. 1, January 1969, pp. 55-66.

(6) Ong, C.M., and Lipo, T.A., "An Approach to Closed Loop Design of a Current Source Inverter/Reluctance Motor Drive System", to be presented at the 1975 IEEE-IAS Annual Meeting, Sept. 28-Oct. 2, 1975.

(7) Ward, E.E., "Inverter Suitable for Operation over a Range of Frequency", Proc. IEE, Vol. III, No. 8, Aug. 1964, pp. 1423-1434.

(8) Williamson, A.C., "Calculation of Saturation Effects in Segmented-Rotor Reluctance Machines", Proc. IEE, Vol. 121, No. 10, Oct. 1974, pp. 1127-1133.

(9) Slemon, G.R., Dewan, S.R. and Wilson, J.W.A., "Synchronous Motor Drive with Current-Source Inverter", IEEE-IAS, Conf. Record, 1973, pp. 875-879.

(10) Krause, P.C. and Lipo, T.A., "Analysis and Simplified Representations of Rectifier-Inverter Reluctance-Synchronous Motor Drives", IEEE Trans. PAS, Vol. 88, June 1969, pp. 962-940.

Appendix I

The linear equations describing the small excursion from a nominal load condition may be obtained by considering small perturbation of the system equations. The subscript 'I' is omitted from the torque angle δ_I. The subscript 'o' is used to denote the steady-state or "operating point" value of the variable.

The perturbation equations for an inductance machine have been derived in Ref. 2. Note that in Eqs. 26-33, the rotor currents are expressed in a rotor reference frame whereas the stator voltage and current has been referred to the synchronously rotating frame. Assuming $\Delta i_{qs}^e = 0$ the perturbation equations are

$$\begin{aligned}\Delta v_{ds}^e = {} & (x_{ds}\cos^2\delta_o + x_{qs}\sin^2\delta_o)\frac{p}{\omega_b}\Delta i_{ds}^e \\ & - (x_{ds} - x_{qs}) i_{dso}^e \frac{\sin 2\delta_o}{2}\frac{p}{\omega_b}\Delta\delta \\ & + x_{ad}\cos\delta_o \frac{p}{\omega_b}\Delta i_{dr}'^r - x_{aq}\sin\delta_o \frac{p}{\omega_b}\Delta i_{qr}'^r + r_s\Delta i_{ds}^e \\ & - (x_{ds} - x_{qs}) i_{dso}^e \frac{\sin 2\delta_o}{2}\frac{\Delta\omega_r}{\omega_b} \\ & - \frac{\omega_{ro}}{\omega_b}(x_{ds} - x_{qs})\frac{\sin 2\delta_o}{2}\Delta i_{ds}^e \\ & - \frac{\omega_{ro}}{\omega_b}(x_{ds} - x_{qs})\, i_{dso}^e \cos 2\delta_o\, \Delta\delta \\ & - \frac{\omega_{ro}}{\omega_b} x_{aq}\cos\delta_o\, \Delta i_{qr}'^r - \frac{\omega_{ro}}{\omega_b} x_{ad}\sin\delta_o\, \Delta i_{dr}'^r \end{aligned} \tag{25}$$

$$\begin{aligned}\Delta v_{qs}^e = {} & (x_{ds} - x_{qs})\frac{\sin 2\delta_o}{2}\frac{p}{\omega_b}\Delta i_{ds}^e \\ & + x_{ad}\sin\delta_o \frac{p}{\omega_b}\Delta i_{dr}'^r + x_{aq}\cos\delta_o \frac{p}{\omega_b}\Delta i_{qr}'^r \end{aligned}$$

$$- (x_{ds}\sin^2\delta_o + x_{qs}\cos^2\delta_o)\, i^e_{dso}\, \frac{p}{\omega_b}\,\Delta\delta + (x_{qs}\sin^2\delta_o + x_{ds}\cos^2\delta_o)\, i^e_{dso}\, \frac{\Delta\omega_r}{\omega_b} + \frac{\omega_{ro}}{\omega_b}(x_{qs}\sin^2\delta_o + x_{ds}\cos^2\delta_o)\Delta i^e_{ds} + \frac{\omega_{ro}}{\omega_b}(x_{qs} - x_{ds})\, i^e_{dso}\sin 2\delta_o\,\Delta\delta + \frac{\omega_{ro}}{\omega_b}\, x_{ad}\cos\delta_o\,\Delta i'^r_{dr} - \frac{\omega_{ro}}{\omega_b}\, x_{aq}\sin\delta_o\,\Delta i'^r_{qr} \quad (26)$$

$$0 = -x_{ad}\, i^e_{dso}\sin\delta_o\,\frac{p}{\omega_b}\Delta\delta + x_{ad}\cos\delta_o\,\frac{p}{\omega_b}\,\Delta i^e_{ds} + x'_{dr}\,\frac{p}{\omega_b}\,\Delta i'^r_{dr} + r'_{dr}\,\Delta i'^r_{dr} \quad (27)$$

$$0 = -x_{aq}\, i^e_{dso}\cos\delta_o\,\frac{p}{\omega_b}\,\Delta\delta - x_{aq}\sin\delta_o\,\frac{p}{\omega_b}\,\Delta i^e_{ds} + x'_{qr}\,\frac{p}{\omega_b}\,\Delta i'^r_{qr} + r'_{qr}\Delta i'^r_{qr} \quad (28)$$

$$\Delta T_e = -(x_{ad} - x_{aq})\, i^e_{dso}\sin 2\delta_o\,\Delta i^e_{ds} - (x_{ad} - x_{aq})(i^e_{dso})^2\cos 2\delta_o\,\Delta\delta - x_{ad}\, i^e_{dso}\sin\delta_o\,\Delta i'^r_{dr} - x_{aq}\, i^e_{dso}\cos\delta_o\,\Delta i'^r_{qr} \quad (29)$$

$$\Delta V'_R = \Delta v^e_{ds} + (R'_F + X'_F\,\frac{p}{\omega_b})\Delta i^e_{ds} \quad (30)$$

$$2Hp\,\frac{\Delta\omega_r}{\omega_b} = \Delta T_e - \Delta T_L \quad (31)$$

$$p\Delta\delta = \Delta\omega_r - \Delta\omega_e \quad (32)$$

These equations can be written in matrix form as

$$\begin{bmatrix} (X'_F + x_{ds}\cos^2\delta_o + x_{qs}\sin^2\delta_o) & x_{ad}\cos\delta_o & -x_{aq}\sin\delta_o & 0 & 0 \\ x_{ad}\cos\delta_o & x'_{dr} & 0 & 0 & 0 \\ -x_{aq}\sin\delta_o & 0 & x'_{qr} & 0 & 0 \\ 0 & 0 & 0 & 1 & 0 \\ 0 & 0 & 0 & 0 & -2H\omega_b \end{bmatrix} \cdot \frac{p}{\omega_b} \begin{bmatrix} \Delta i^e_{ds} \\ \Delta i'^r_{dr} \\ \Delta i'^r_{qr} \\ \Delta\delta \\ \frac{\Delta\omega_r}{\omega_b} \end{bmatrix} = \begin{bmatrix} [r_s + R'_F - \frac{\omega_{ro}}{\omega_b}(x_{ds} - x_{qs})\frac{\sin 2\delta_o}{2}] & -\frac{\omega_{ro}}{\omega_b}x_{ad}\sin\delta_o & -\frac{\omega_{ro}}{\omega_b}x_{aq}\cos\delta_o \\ 0 & r'_{dr} & 0 \\ 0 & 0 & r'_{qr} \\ 0 & 0 & 0 \\ -i^e_{dso}(x_{ds} - x_{qs})\sin 2\delta_o & -i^e_{dso}x_{ad}\sin\delta_o & -i^e_{dso}x_{aq}\cos\delta_o \end{bmatrix}$$

$$\begin{bmatrix} -i^e_{dso}(x_{ds} - x_{qs})\cos 2\delta_o & -i^e_{dso}(x_{ds} - x_{qs})\sin 2\delta_o \\ 0 & -i^e_{dso}\, x_{ad}\sin\delta_o \\ 0 & -i^e_{dso}\, x_{aq}\cos\delta_o \\ 0 & -1 \\ -(i^e_{dso})^2(x_{ds} - x_{qs})\cos 2\delta_o & 0 \end{bmatrix} \cdot \begin{bmatrix} \Delta i^e_{ds} \\ \Delta i'^r_{dr} \\ \Delta i'^r_{qr} \\ \Delta\delta \\ \frac{\Delta\omega_r}{\omega_b} \end{bmatrix} - \begin{bmatrix} -1 & 0 & (x_{ds} - x_{qs})\, i^e_{dso}\,\frac{\sin 2\delta_o}{2} \\ 0 & 0 & i^e_{dso}\, x_{ad}\sin\delta_o \\ 0 & 0 & i^e_{dso}\, x_{aq}\cos\delta_o \\ 0 & 0 & 1 \\ 0 & -1 & 0 \end{bmatrix} \cdot \begin{bmatrix} \Delta V'_R \\ \Delta T_L \\ \frac{\Delta\omega_e}{\omega_b} \end{bmatrix} \quad (33)$$

Appendix II

Motor Parameters	Per Unit Value
r_s	0.045
r'_{qr}	0.015
r'_{dr}	0.030
$x_{\ell s}$	0.100
$x'_{\ell dr}$	0.100
$x'_{\ell qr}$	0.100
x_{aq}(unsat)	0.500
x_{ad}(unsat)	2.000
H (inertia constant)	0.400 (S)
R_F	0.100
X_F	1.2

Both quantities are peak-to-peak values of the machine phase voltage and line current[10]. Base frequency, $\omega_b/2\pi$, is 60 Hz.

Appendix III

Conditions for Maximum Steady-State Torque

When rectifier voltage is held constant, dropping the 'o' subscript for simplicity

$$V'_R = I'_R R'_F + I'_R \left[r_s - f_R(x_{ds} - x_{qs}) \frac{\sin 2\delta_I}{2} \right] \quad (34)$$

The average electromagnetic torque developed by the machine is given by

$$T_e = -I'^2_R (x_{ds} - x_{qs}) \frac{\sin 2\delta_I}{2} \quad (35)$$

Combining these two equations

$$V'_R I'_R = I'^2_R (R'_F + r_s) + f_R T_e \quad (36)$$

Since $I_R > 0$, Eq. 36 can be solved as

$$I'_R = \frac{V'_R + \sqrt{V'^2_R - 4(R'_F + r_s) f_R T_e}}{2(R'_F + r_s)} \quad (37)$$

The dc link current I_R must also be real. Hence, the maximum torque for a given operating frequency is

$$T_{LIM} = \frac{V'^2_R}{4f_R(R'_F + r_s)} \quad (38)$$

at which point

$$I'_R = \frac{V'_R}{2(R'_F + r_s)} \quad (39)$$

Equation 38 defines the upper limit to the region of permissible steady-state operation for a fixed rectifier voltage and corresponds to the negatively sloped portion of the stability regions in Figs. 9, 11 and 12. If Eq. 36 is differentiated with respect to I'_R it can be shown that Eq. 38 corresponds to a maximum power limitation. At sufficiently low frequencies the upper limit becomes defined by a torque limit rather than a power limit. The transition point occurs when the maximum torques in the two regions are equated. Setting $\delta_I = 45°$ in Eq. 35 and equating to 38 we have

$$I'^2_R \frac{(x_{ds} - x_{qs})}{2} = \frac{V'^2_R}{4f_R(R'_F + f_s)} \quad (40)$$

However, the transition point I'_R is also defined by Eq. 39 so that Eq. 40 reduces to

$$\frac{x_{ds} - x_{qs}}{8(R'_F + r_s)^2} \quad \frac{1}{4f_R(R'_F + r_s)} \quad (41)$$

Hence, the transition point between torque limited and power limited operation is defined by

$$f_R = \frac{2(R'_F + r_s)}{x_{ds} - x_{qs}} \quad (42)$$